A Journal of the Gesellschaft Deutscher Chemiker

Angewandte International Edition

GDCh

Chemie

www.angewandte.org

Accepted Article

Title: Hybrid Co Quaterpyridine Complex /Carbon Nanotube Catalytic Material for CO2 Reduction in Water

Authors: Marc Robert, Tai-Chu Lau, Min Wang, and Lingjing Chen

To be cited as: *Angew. Chem. Int. Ed.* 10.1002/anie.201802792
Angew. Chem. 10.1002/ange.201802792

Link to VoR: http://dx.doi.org/10.1002/anie.201802792
http://dx.doi.org/10.1002/ange.201802792

WILEY-VCH

10.1002/anie.201802792

WILEY-VCH

Hybrid Co Quaterpyridine Complex /Carbon Nanotube Catalytic Material for CO_2 Reduction in Water

Min Wang,[a] Lingjing Chen,[b] Tai-Chu Lau*[c] and Marc Robert*[a]

Abstract: Associating a molecular earth-abundant metal based catalyst to a carbon based nanomaterial is a promising approach for the production of solar fuels from CO_2. Upon appending a Co(II) quaterpyridine complex $[Co(qpy)]^{2+}$ at the surface of multi-walled carbon nanotubes, CO_2 conversion into CO was realized in water at pH 7.3 with 100% catalytic selectivity and 100% Faradaic efficiency, at low catalyst loading and reduced overpotential. A current density of 0.94 mA cm^{-2} was reached at -0.35 V vs. RHE (240 mV overpotential), and 9.3 mA cm^{-2} could be sustained for hours at only 340 mV overpotential with excellent catalyst stability, leading to 89 095 catalytic cycles within 4.5 h, while 19.9 mA cm^{-2} was met at 425 mV overpotential. Such hybrid material combines the high selectivity of a homogeneous molecular catalyst to the robustness of a heterogeneous material. Catalytic performances compare well with those of noble metal based metallic nano-electrocatalysts as well as atomically dispersed metal atoms in carbon matrices.

Tremendous efforts are currently devoted to convert solar energy into storable chemical forms, for example by catalyzing CO_2 reduction into fuels.[1-3] Molecular catalysts have been developed to this aim. Focusing on earth abundant metals, a number of 3d complexes based on Mn, Fe, Co and Ni have been reported.[4-5] These catalysts are mainly active in aprotic solvent with reaction products being mostly CO and more rarely HCOOH. CO_2 reduction catalysts operating in aqueous conditions remain scarce, in particular because of low CO_2 concentration and competing H_2 evolution. Ni cyclam was first reported as a selective and efficient catalyst of the CO_2-to-CO conversion in water at a mercury surface electrode, with favorable specific interactions of the catalytic adsorbed species with the surface,[6-7] while the use of a carbon electrode leads to much less efficiency in terms of rate (maximal turnover frequency of 90 s^{-1}) and turnover (4 cycles).[8] Another recent example is given by a tetraphenyl Fe porphyrin with trimethyl ammonio groups appended at the para position of the four phenyl groups.[9-10] In that case, CO production was achieved with over 90% selectivity at neutral pH and a moderate 450 mV overpotential. Formate production has been even more rare, with as example small iron clusters, such as $[Fe_4N(CO)_{12}]^-$ reaching selectivity and Faradaic efficiency (FE) above 95%, while the applied overpotential for the reaction is only 230 - 440 mV (pH 7 – 13) [11] Another strategy entails adsorbing an insoluble catalyst at the surface of a conductive electrode. Towards this goal, various carbon supports including glassy carbon, pyrolytic graphite, nanotube, graphene have been recently used. Among several examples, Fe[12] and Co[13-15] porphyrins as well as Co phthalocyanines[16-17] have been investigated. These latter compounds are catalysts of choice with excellent activity for CO production, leading to selectivity above 90% at overpotential larger than 500 mV and current in the range of 10 mA cm^{-2}. These performances remain below those of noble metal based nanomaterials, notably state-of-the art gold nanoneedles,[18] but it however opens very interesting perspectives since these hybrid systems only contain earth abundant elements and the catalyst structure could be tuned to reach even better selectivity and higher intrinsic activity.

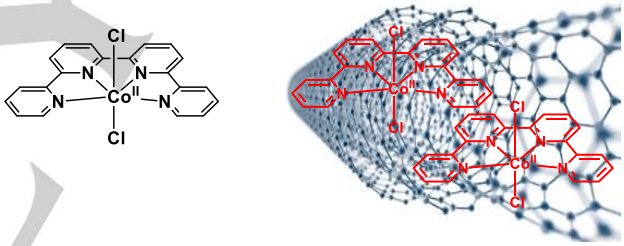

Scheme 1. Structure of the molecular complex catalyst $[Co(qpy)](Cl)_2$ (left) and schematic view of the hybrid material (**$[Co(qpy)]^{2+}$**@MWCNTs, right).

We have recently reported that Co complex of the planar tetradentate ligand 2,2':6',2'':6'',2'''-quaterpyridine (noted $[Co(qpy)]^{2+}$, Scheme 1) is an active catalyst for both the photocatalytic[19] and electrochemical[20] reduction of CO_2 in aprotic solvent, with the formation of CO in high yield and with good selectivity. In electrochemical conditions, we have shown that the doubly reduced Co complex could activate the CO_2 in the presence of a weak acid, like e.g. phenol, with 94% Faradaic efficiency at overpotential as low as 140 mV. Such promising properties prompted us to investigate catalysis in water solutions, by appending the catalyst at the surface of a conductive carbon material. To do so, we first prepare an ink from a suspension of carbon nanotube and the catalyst to ensure good electronic conduction, which was further deposited onto various solid supports (glassy carbon or carbon paper).

Briefly, the catalytic inks were prepared by dispersing the multi-walled carbon nanotubes (MWCNTs) in 1:1 mixture of ethylene glycol and ethanol. After sonication, the $[Co(qpy)]^{2+}$ catalyst was added to the carbon colloidal suspension, before addition of a small amount of Nafion®. The ink was stirred for 24h prior use. Typical catalyst loading was 10^{-8} - 10^{-9} mol per cm^2 of electrode and the material was drop-casted either onto

[a] Ms M., Wang, Prof., Dr. M., Robert
Université Paris Diderot, Sorbonne Paris Cité, Laboratoire d'Electrochimie Moléculaire, Unité Mixte de Recherche Université–CNRS no. 7591, Bâtiment Lavoisier, 15 rue Jean de Baïf, 75025 Paris Cedex 13, France
E-mail: robert@univ-paris-diderot.fr
[b] Dr. L., Chen
School of Environmental and Civil Engineering
Dongguan University of Technology
Guangdong 523808, P. R. China
[c] Prof., Dr. T.-C., Lau
Department of Chemistry and Institute of Molecular Functional Materials
City University of Hong Kong,
Tat Chee Avenue, Kowloon, Hong Kong, P. R. China
E-mail: bhtclau@cityu.edu.hk

Supporting information for this article is given via a link at the end of the document.

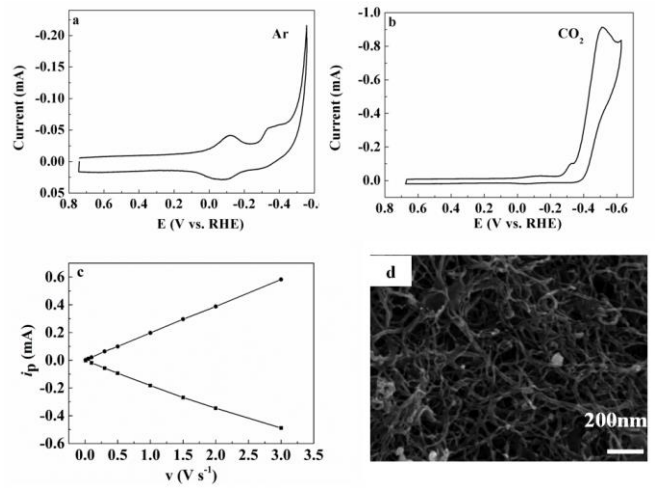

Figure 1. Cyclic voltammetry of a **[Co(qpy)]$^{2+}$**@MWCNTs film deposited onto a glassy carbon electrode (*d* = 3 mm) in $NaHCO_3$ 0.5 M at *v* = 0.1 V/s under argon (a, pH = 8.5) and CO_2 (b a, pH = 7.3). Variation of the peak current vs. scan rate for the Co^{II}/Co^{I} redox wave (c) and SEM image of a catalytic film deposited onto carbon paper (d).

glassy carbon (S = 0.07 cm^2, cyclic voltammetry) or porous carbon paper (S = 1 or 0.5 cm^2, electrolysis). A constant CO_2 flux was maintained through the solution during electrolysis to avoid as much as possible limitation from gas diffusion and the gas was circulated through a glass frit to generate small sized bubbles in order to increase contact surface with the liquid phase (Figure S1). Uncompensated ohmic drop was ca. 3 Ω with our set-up and current densities are reported in the text as a function of the geometric surface area of the working electrode.

Typical cyclic voltammetry of a catalytic film under Ar and then under CO_2 is shown in Figure 1. The Co^{II}/Co^{I} reversible reduction wave was observed with peak potential close to -0.16 V vs. RHE. As expected for a surface confined wave, the peak current was proportional to the scan rate up to 3 V s^{-1} (Figure 1c). The concentration of $[Co(qpy)]^{2+}$ could be obtained from surface integration of the wave or from the variation of the peak current with the scan rate, leading to 2.86 nmol cm^{-2}. Since the totally added catalyst was 16 nmol cm^{-2}, it indicates that only 18% is electrochemically active within the film (Figure S2). Scanning electron microscopy of the film (Figure 1d) shows the dense network of carbon nanotubes with some porosity; it is likely that high catalyst loading will lead to incomplete dispersion (upon aggregate formation) or surface saturation and thus to lower electrochemical activity than expected. A second reduction irreversible reduction wave, likely centered on the ligand was observed at ca. -0.36 V vs. RHE. Upon CO_2 saturation of the solution, a large catalytic wave appears at -0.53 V vs RHE (Figure 1b). It indicates that the CO_2 binds to the doubly reduced Co complex, leading to CO production upon protonation and further reduction of the adduct. A Tafel plot gave a slope of 120 mV dec^{-1} (Figure S3), pointing towards an electron step as rate determining, although mass transport may also intervene in the kinetics. Further mechanistic analysis of the film, notably by voltammetry, will be reported in due time.

Table 1. Catalytic performances during bulk electrolysis (*E* = -0.48 V vs. RHE) for a **[Co(qpy)]$^{2+}$**@MWCNTs film in a CO_2 saturated solution containing 0.5 M $NaHCO_3$ (pH 7.3).

t (s)	Catalyst loading (nmol cm^{-2})[a]	Current density (mA cm^{-2})	Number of catalytic cycles	TOF (s^{-1})	CO selectivity (%)
12 550	20.5[b]	6.3	42 960	3.4	100
23 300	20.5[b]	6.8	79 810	3.4	100
5 000	17.5[b]	7.6	19 310	3.8	100
5 000	8.5	10.0	29 360	5.9	100
5 000	3.4	5.4	41 330	8.2	100
5 000	1.0	2.0	52 590	10.5	100
5 000	0.5	0.65	34 160	6.8	100
16 200	8.5	9.3	89 095	5.45	100
5 000	8.5	11.8[c]	35 875	7.2	100
5 000	8.5	19.9[d]	59 910	12.0	99

a. total amount of catalyst added in the film.
b. at these loadings, the electroactive concentration of the cobalt catalyst could be estimated from the linear CV prior to electrolysis, showing that only ca. 60% of the initial deposited complex is active within the film (see Fig. 2). Entries 1 and 2 correspond to two separate experiments (see text).
c. *E* = -0.53 V vs. RHE. d. *E* = -0.58 V vs. RHE

Encouraged by these observations, an electrolysis was performed at -0.48 V vs. RHE after depositing 20.5 nmol of catalyst onto the porous 1 cm^2 carbon electrode. Active catalyst was estimated to equal 11.4 nmol from linear scan voltammetry (Figure S4), highlighting the electrode porosity positive impact as compared to the glassy carbon used in cyclic voltammetry. As seen from Figure 2a, a high and stable current density of 6.3 mA cm^{-2} was obtained during 3.5h, with excellent selectivity (ca. 100%) and Faradaic efficiency (ca. 100%), with only traces of H_2. It corresponds to a turnover frequency (TOF) of 3.4 s^{-1} and a turnover number (TON) of 42 960 (Table 1, entry 1). Note that blank experiment in the absence of $[Co(qpy)]^{2+}$ led to residual current (0.07 mA cm^{-2}) and 21% FE for CO production, corresponding to a partial current of 0.015 mA cm^{-2} (Figure S5a). X-ray photoelectron spectroscopy (XPS) interrogation of the surface revealed the cobalt $2p_{1/2}$ peaks and $2p_{3/2}$ peaks at 782.5 eV and 797.5 eV respectively, as well as nitrogen 1s peak at 399.4 eV, with no change before and after the 3.5h electrolysis, confirming the molecular nature of the catalyst within the film (Figure S5b-c). Linear scan voltammetry of the film and UV-Vis absorption spectra of the solution performed before and after electrolysis were identical (Figure S6a-b). An additional electrolysis with a non-coated carbon paper electrode in the electrolyte solution used described above led to the absence of any CO production, further ruling out the release of Co species in the solution during electrolysis with catalytic film (Figure S6c-d). As shown from Figure 2b, film catalytic activity is highly reproducible and could be extended to longer electrolysis time with sustained CO production for 6.5h and a TON of 79 810

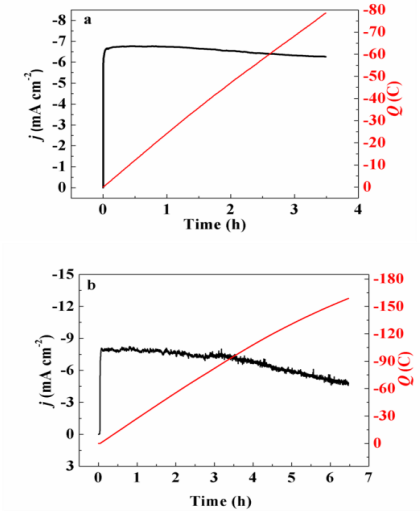

Figure 2. Current and charge evolved during bulk electrolysis (E = -0.48 V vs. RHE) of a CO_2 saturated solution containing 0.5 M $NaHCO_3$ (pH 7.3) for a **[Co(qpy)]$^{2+}$**@MWCNTs film deposited at a 1 cm^2 porous carbon paper (electroactive Co surface concentration was Γ = 11.4 10^{-9} mol cm^{-2} (a) and Γ = 12.4 10^{-9} mol cm^{-2} (b) from 20.5 10^{-9} mol cm^{-2} catalyst added in the film).

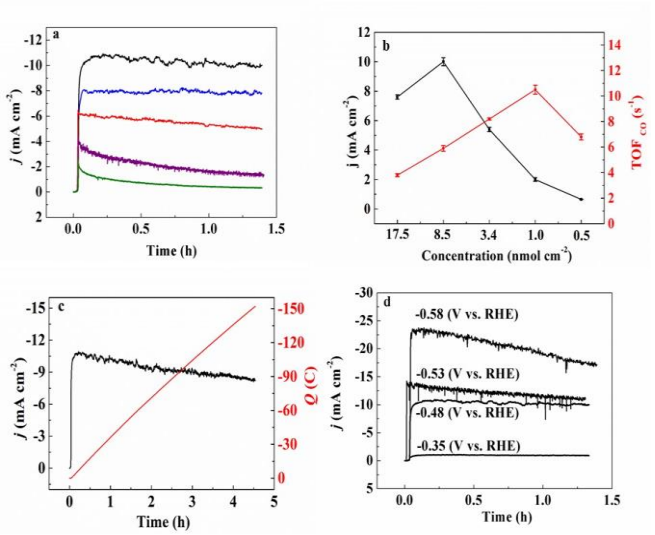

Figure 3. Bulk electrolysis (E = -0.48 V vs. RHE) current of a CO_2 saturated solution containing 0.5 M $NaHCO_3$ (pH 7.3) for a **[Co(qpy)]$^{2+}$**@MWCNTs film at various catalyst loading ($\Gamma_{deposited}$ = 1.75 10^{-8} mol cm^{-2} (blue), 8.5 10^{-9} mol cm^{-2} (black), 3.4 10^{-9} mol cm^{-2} (red), 1 10^{-9} mol cm^{-2} (purple), 5 10^{-10} mol cm^{-2} (green)) (a). Current density and rate constant (TOF) for CO production as a function of catalyst loading (b). Long term electrolysis (E = -0.48 V vs. RHE) (c) and variation of the current as a function of electrolysis potential at optimized catalyst loading (Γ = 8.5 10^{-9} mol cm^{-2}) (d).

(Table 1, compare entry 1 and entry 2).

The catalyst loading effect was further investigated and the [Co(qpy)]$^{2+}$ initial concentration was decreased from 20.5 nmol cm^{-2} down to 0.5 nmol cm^{-2} (Table 1, entries 1-7). In these experiments, the amount of MWCNTs was kept constant while the Co catalyst concentration was progressively diminished in the ink composition. Whatever the loading, both selectivity and efficiency for CO_2 reduction kept perfect (Table 1). Remarkably, the current density first increases upon decrease of catalyst concentration, reaching a maximum value of 10 mA cm^{-2} at a loading of 8.5 nmol cm^{-2} (Figure 3a and Table 1, entry 4) and it then decreases with a value of 0.65 mA cm^{-2} at 5 10^{-10} nmol cm^{-2}. The maximum current density corresponds to the optimized ratio between the catalyst loading and the fraction being catalytically active in the film. Interestingly, the TOF continuously increases with catalyst lessening until 1 nmol cm^{-2} with a maximum value of 10.5 s^{-1} (Table 1, entry 6), the highest rate so far obtained for a molecular catalyst in a conductive film. At the smallest loading investigated (0.5 nmol cm^{-2}), the TOF slightly decreases (6.8 s^{-1}, Table 1, entry 7), while the current decreases quickly over time (Figure 3a), reflecting some degradation of the catalyst that affect the performance. Using the optimized [Co(qpy)]$^{2+}$ concentration in the film (8.5 nmol cm^{-2}), a long term electrolysis was performed for 4.5 h (Figure 3c). An average current of 9.3 mA cm^{-2} was sustained, corresponding to 89 095 TON for CO and a TOF value of 5.45 s^{-1} (Table 1, entry 8). It corresponds to a mass activity of 2.48 A/mg of Co catalytst and the overpotential η in these conditions was 340 mV (taking into account a 30 mV ohmic drop) since the apparent standard redox potential E^0(CO_2/CO) = -0.11 V vs. RHE at pH 7.3. Upon increasing the electrolysis potential to -0.25 V vs. RHE, which corresponds to a low 240 mV overpotential, extremely stable current was obtained with an average 0.94 mA cm^{-2} (TOF 0.59 s^{-1}, 100% CO; see Figure 3d). Conversely, applying an overpotential of ca. 385 mV (E = -0.53 V vs. RHE) led to an average current of 11.9 mA cm^{-2} during 1.3 h (TOF 7 s^{-1}) as illustrated in Figure 3d, with again complete conversion of the CO_2 into CO only (Table 1, entry 9). At more negative E = -0.58 V vs RHE, 1% H_2 was formed as a side product alongside CO (99% efficiency), and an average current density of 19.9 mA cm^{-2} was sustained (Table 1, entry 10) but a decrease was observed, likely due to limitation by the CO_2 gas diffusion and/or proton availability, and/or some degradation of the catalyst (Figure 3d and Figure S7).

Remarkably, the heterogenized [Co(qpy)]$^{2+}$ competes well with the best performances so far obtained with molecular catalysts for CO_2 conversion in water both in terms of selectivity, rate and overpotential (Table 2). As mentioned in the introduction, such catalysts include Co tetraphenyl porphyrin (CoTPP) adsorbed onto carbon nanotube that gives ca. 3.2 mA cm^{-2} at 550 mV overpotential and a selectivity of 91% at a surfacic concentration ca. 3 times larger than ours (Table 2, entry 3).[15] Co phthalocyanines have also been investigated recently when adsorbed[16] or polymerized around carbon nanotubes.[17] In the latter case, a maximum TOF of 1.4 s^{-1} at 500 mV overpotential with 90% Faradaic efficiency was obtained, and a current density of 20 mA cm^{-2} was measured for a loading of 1 mg cm^{-2}, 13 times larger than in our optimized conditions (Table 2, entry 5, CoPpc). In the former case, substituted Co phthalocyanine with 8 cyano groups led to 5.6 mA cm^{-2} at 340 mV overpotential (TOF 1.4 s^{-1}) and 88% CO selectivity, while an optimized CO selectivity of 98% (TOF of 4.1 s^{-1}) was obtained at 520 mV overpotential with a catalyst loading more than 5 times larger than ours (Table 2, entry 4, CoPc-CN). Moreover, [Co(qpy)]$^{2+}$ also closely matches some of the most active solid electrocatalysts, including noble metals. A recent class of emerging catalytic materials is given by graphene type materials

Table 2. Comparison of the Coqpy/MWCNTs hybrid catalyst with previously reported state-of-the art immobilized molecular catalysts and Au nanomaterial.

Catalyst	Film loading (mg cm^{-2})	Overpotential (mV)	Current density (mA cm^{-2})	TOF (s^{-1})	CO selectivity (%)
Coqpy[a]	0.08	340	10.0	5.9	100
Coqpy[a]	0.08	425	19.9	12	99
CoTPP[15]	0.25	550	3.2	0.08	91
CoPc-CN[16]	0.4	520	~ 15.0	4.1	98
CoPpc[17]	~ 1	500	20	1.4	~ 90
Au nanoneedles[18]	/	240	22	/	> 95

a: this work.

with atomically dispersed metal atoms, including notably Ni[21-22] and Co.[23] With cobalt, CO selectivity up to 94% was obtained at 520 mV overpotential (TOF 5 s^{-1}) with a current density of 18 mA cm^{-2}, while comparable performances were recently achieved using nickel with selectivity in the range of 95% and current density from 10 to 22 mA cm^{-2} (TOF from 4.1 to 6.8 s^{-1}) at overpotential close to 600 mV. Regarding noble metals, nanostructured silver catalyst can achieve 9 mA cm^{-2} (90% selectivity) at 390 mV overpotential.[24] Oxide-derived Au nanoparticles can furnish 10 mA cm^{-2} at only 260 mV overpotential,[25] while state-of-the art gold nanoneedles give a CO current up to 22 mA cm^{-2} at only 240 mV overpotential (Table 2, entry 6).[18]

In conclusion, $[Co(qpy)]^{2+}$, when combined to a conductive material like e.g. multi-walled carbon nanotubes, is a highly efficient supported homogeneous catalyst for the conversion of CO_2 to CO in water at neutral pH and with very low overpotential. It reaches perfect catalytic selectivity and unity Faradaic efficiency in the explored potential window (from -0.35 to -0.58 V vs. RHE). The ability of the catalyst to be reduced with 2 electrons and then to bind CO_2 at weakly negative potentials is a key to its exceptional selectivity. The hybrid catalytic material is also stable over long period of time and current densities from 1 mA cm^{-2} to ca. 19.9 mA cm^{-2} could be sustained with overpotential varying from ca. 240 mV to 425 mV respectively. A lot remains to be done to further explore this type of materials, including optimizing the conductive support as well as the film composition, and most importantly deciphering the mechanism within the supported films. Such studies are currently in progress. It may then be included in flow cell with gas diffusion electrodes to reach higher current densities. Finally, this work highlights the fact that hybrid systems comprising a simple molecular catalyst including earth abundant metal associated to a carbon porous conductive support may rival the performances of the most active solid materials, including atomically dispersed metal atoms in carbon matrices and noble metal based nanomaterials.

Acknowledgements

The work described in this project was supported by the Hong Kong University Grants Committee Area of Excellence Scheme (AoE/P-03-08), the CityUniversity of Hong Kong (7004399 and 9680174), the National Science Foundation of China (No. 21703034) and the *Institut Universitaire de France* (IUF). PhD fellowship to M. W. from China Scholarship Council (CSC, grant number 201606220034) is gratefully acknowledged.

Keywords: • electrochemical catalysis • carbon dioxide reduction• Co complex • supported heterogeneous catalysis • hybrid materials •

[1] H.-R. M. Jhong, S. Ma, P. J. Kenis, *Curr. Opin. Chem. Eng.* **2013**, *2*, 191-199.
[2] Z. W. Seh, J. Kibsgaard, C. F. Dickens, I. Chorkendorff, J. K. Nørskov, T. F. Jaramillo, *Science* **2017**, *355*, eaad4998.
[3] A. Tatin, J. Bonin, M. Robert, *ACS Energy Lett.* **2016**, *1*, 1062-1064.
[4] R. Francke, B. Schille, M. Roemelt, *Chem. Rev.* **2018**, Advance Article, DOI: 10.1021/acs.chemrev.7b00459 and references therein.
[5] H. Takeda, C. Cometto, O. Ishitani, M. Robert, *ACS Catal.* **2017**, *7*, 70-88 and references therein.
[6] M. Beley, J. P. Collin, R. Ruppert, J. P. Sauvage, *Chem. Commun.* **1984**, 1315-1316.
[7] M. Beley, J. P. Collin, R. Ruppert, J. P. Sauvage, *J. Am. Chem. Soc.* **1986**, *108*, 7461-7467.
[8] J. D. Froehlich. C. P. Kubiak, *Inorg. Chem.* **2012**, *51*, 3932-3934.
[9] C. Costentin, M. Robert, J-M. Savéant, A. Tatin, *Proc. Natl. Acad. Sci. USA* **2015**, *112*, 6882-6886.
[10] A. Tatin, C. Cominges, B. Kokoh, C. Costentin, M. Robert, J-M. Savéant, *Proc. Natl. Acad. Sci. USA* **2016**, *113*, 5526-5529.
[11] A. Taheri, L. A. Berben, *ACS Catal.*, **2015**, *5*, 7140-7515.
[12] A. Maurin, M. Robert, *J. Am. Chem. Soc.* **2016**, *138*, 2492-2495.
[13] J. Shen, R. Kortlever, R. Kas, Y. Y. Birdja, O. Diaz-Morales, Y. Kwon, I. Ledezma-Yanez, K. J. P. Schouten, G. Mul, M. T. M. Koper, *Nat. Commun.* **2015**, 6:8177.
[14] S. Aoi, K. Mase, K. Ohkubo, S. Fukuzumi, *Chem. Commun.* **2015**, *51*, 10226-10228.
[15] X-M. Hu, M. H. Ronne, S. U. Pedersen, T. Skrydstrup, K. Daasbjerg, *Angew. Chem. Int. Ed.* **2017**, 56, 6468-6472.
[16] X. Zhang, Z. Wu, X. Zhang, L. Li, Y. Li, H. Xu, X. Li, X. Yu, Z. Zhang, Y. Liang, H. Wang, *Nat. Commun.* **2017**, 8:14675.
[17] N. Han, Y. Wang, L. Ma et al., *Chem* **2017**, *3*, 652-664.
[18] M. Liu, Y. Pang, B. Zhang, P. De Luna et al., *Nature* **2016**, *537*, 382-386.
[19] Z. Guo, S. Cheng, C. Cometto, E. Anxolabéhère-Mallart, S-M. Ng, C-C. Ko, G. Liu, L. Chen, M. Robert, T-C. Lau, *J. Am. Chem. Soc.* **2016**, *138*, 9413–9416.
[20] C. Cometto, L. Chen, P-K. Lo, Z. Guo, K-C. Lau, E. Anxolabéhère-Mallart, C. Fave, T-C. Lau, M. Robert, *ACS Catal.* **2018**, 4, 3411-3417.
[21] K. Jiang, S. Siahrostami, T. Zheng, Y. Hu, S. Hwang, E. Stavitski, Y. Peng, J. Dynes, M. Gangisetty, D. Su, K. Attenkofer, H. Wang, *Energy Environ. Sci.*, **2018**, Advance Article, DOI: 10.1039/C7EE03245.
[22] H. B. Yang, S-F. Hung, S. Liu et al., *Nature Cat.* **2018**, *3*, 140-147.
[23] X. Wang, Z. Chen, X. Zhao et al., *Angew. Chem. Int. Ed.* **2018**, 57, 1944-1948.
[24] Q. Lu, J. Rosen, Y. Zhou, G. S. Hutchings, Y. C. Kimmel, J. G. Chen, F. Liao, *Nat. Commun.* **2014**, 5:3242.
[25] Y. Chen, C. W. Li, M. W. Kanan, *J. Am. Chem. Soc.* **2012**, *134*, 19969-19972.

10.1002/anie.201802792

WILEY-VCH

Entry for the Table of Contents (Please choose one layout)

Layout 1:

COMMUNICATION

Text for Table of Contents

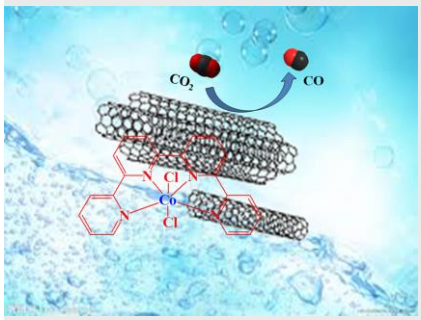

*Author(s), Corresponding Author(s)**

Page No. – Page No.

Title